Convergence analysis of the Newton algorithm and a pseudo-time marching scheme for diffuse correlation tomography

Hari M. Varma,[1] B. Banerjee,[2] D. Roy,[2] A. K. Nandakumaran,[3] and R. M. Vasu[1,*]

[1]*Department of Instrumentation, Indian Institute of Science, Bangalore, 560012, India*
[2]*Department of Civil Engineering, Indian Institute of Science, Bangalore, 560012, India*
[3]*Department of Mathematics, Indian Institute of Science, Bangalore, 560012, India*
**Corresponding author: vasu@isu.iisc.ernet.in*

Received September 23, 2009; revised December 14, 2009; accepted December 15, 2009; posted December 15, 2009 (Doc. ID 117652); published January 22, 2010

We propose a self-regularized pseudo-time marching scheme to solve the ill-posed, nonlinear inverse problem associated with diffuse propagation of coherent light in a tissuelike object. In particular, in the context of diffuse correlation tomography (DCT), we consider the recovery of mechanical property distributions from partial and noisy boundary measurements of light intensity autocorrelation. We prove the existence of a minimizer for the Newton algorithm after establishing the existence of weak solutions for the forward equation of light amplitude autocorrelation and its Fréchet derivative and adjoint. The asymptotic stability of the solution of the ordinary differential equation obtained through the introduction of the pseudo-time is also analyzed. We show that the asymptotic solution obtained through the pseudo-time marching converges to that optimal solution provided the Hessian of the forward equation is positive definite in the neighborhood of optimal solution. The superior noise tolerance and regularization-insensitive nature of pseudo-dynamic strategy are proved through numerical simulations in the context of both DCT and diffuse optical tomography.

OCIS codes: 100.3190, 110.6955, 170.0110, 170.3680.

1. INTRODUCTION

We consider the inverse problem of recovery of certain property distributions of a diffuse-scattering object from boundary measurements made on coherent light propagated through it. In diffuse optical tomography (DOT) the absorption (μ_a) and scattering (μ_s) coefficient distributions are recovered from measurement of the photon flux [1,2]. By considering the propagation of the amplitude correlation [$G(\mathbf{r},\tau)$] of light, which is affected by both the optical properties and the dynamics of the scattering particles, in diffuse correlation tomography (DCT) [3] both the mechanical and the optical property distributions can be recovered. In DCT, the boundary measurement is either $G(\mathbf{r},\tau)$ or a quantity related to $G(\mathbf{r},\tau)$, such as the intensity autocorrelation [$g_2(\tau)$] and its moments. The parameter recovered, from which mechanical properties are computed, is the mean-square displacement of scattering centres. Both the DOT and the DCT have important applications in medical diagnostics imaging through their ability to monitor changes in μ_a and the viscoelastic properties that are related to pathological changes.

Our emphasis in this work is the mathematical analysis of the above inverse problem done in the context of DCT. The same analysis holds good for the recovery of μ_a in DOT considering that $G(\mathbf{r},\tau)$ becomes the intensity of light when τ, the correlation time, is zero. We introduce a self-regularized pseudo-dynamic scheme to solve the above inverse problem, which has certain advantages over the usual minimization method employing a variant of the Newton algorithm [4]. The governing equation for the propagation of $G(\mathbf{r},\tau)$ (also referred to as the forward problem) is a partial differential equation [5], the solution of which helps us connect the measurements on the boundary to the parameters of the object. Just as the propagation of photon flux, in DOT, is modeled by using a diffusion equation under the assumption that $\mu_s \gg \mu_a$, the propagation of $G(\mathbf{r},\tau)$ in the context of DCT is also modeled by using a diffusion equation. In the latter, the optical as well as mechanical properties appear as coefficients of the equation [5]. The inverse problem of DCT, which is the recovery of these parameters (the mean-square displacement or D_B, the particle diffusion coefficient, and μ_a, the absorption coefficient distributions) is normally attempted through solving a nonlinear mean-square error minimization problem, which is usually done by using a Newton iteration or one of its variants. The Newton iteration requires the inversion of a locally linearized version of the optimality condition of the minimization problem, which often involves the inversion of an ill-conditioned matrix. To facilitate this inversion, a regularization term [6–8] is added that improves the smoothness and quantitative accuracy of the reconstructed parameter distributions. Apart from the critical dependence of the solution on the regularization parameter, for the selection of which there are computationally expensive procedures, the other disadvantages of the Newton-type algorithms are their divergence in the presence of measurement noise, slow convergence, and the need for a strict stopping criterion.

Some of the difficulties of the deterministic inversion

scheme can be addressed by adopting a stochastic filtering [9] approach which traditionally requires a dynamical systems setting. In keeping with this, the stochastic filtering has been employed to solve the DOT problem when the optical coefficients are dynamically evolving [10]. When the parameters are static, as for example in the static elastography problem, a dynamics evolving in pseudo-time is introduced into the state equilibrium equation [11]. Our present objective in the context of DCT is to consider a pseudo-dynamical (PD) system obtained from the Gauss–Newton update equation, whose integration in time leads to an asymptotic solution of the inverse problem at hand. Since the evolution of the artificial dynamics may be interpreted to be on an invariant Lie manifold, the recursion resulting from integrating the ordinary differential equation (ODE) can have a self-regularized character. Thus one can avoid the explicit use of the regularization while using the PD system approach. In addition, this strategy results in an algorithm that is to a large extent insensitive to measurement noise.

The aim of the present work is twofold: we first show theoretically that the time recursion of the PD strategy has an asymptotic convergence to the solution of the minimization problem. While doing this we also prove rigorously the existence of a minimizer for the objective functional, which can be reached through a Newton iteration. Second, we establish through numerical experiments, done in the context of both the DCT and DOT, the superior performance of the PD recursion *vis-à-vis* the Newton method by bringing forth its noise tolerance in data and regularization-insensitive nature. Since in DCT the measurement on the boundary is the intensity autocorrelation, we also briefly touch on the quick evaluation of the appropriate Jacobian for this measurement.

2. NON-LINEAR LEAST SQUARE ESTIMATION OF VISCOELASTIC COEFFICIENT

When coherent light passes through a tissuelike object, the propagation of amplitude correlation is governed by the partial differential equation [3]

$$\nabla \cdot D \nabla G(\mathbf{r},\tau) - \left(\mu_a + \frac{1}{3}\langle \Delta r^2(\mathbf{r},\tau)\rangle \alpha k_0^2 \mu_s'\right) G(\mathbf{r},\tau) = -q_0(\mathbf{r}-\mathbf{r}_0), \tag{2.1}$$

where k_0 is the modulus of propagation vector of light, $\mu_s'=(1-g)\mu_s$, α is the percentage of light scattered by the moving scatterers, g is the anisotropy factor of scattering, and $D=1/[3(\mu_a+\mu_s')]$ is the optical diffusion coefficient. In the above model, we assume that the scattering is isotropic with a length scale $l^*=1/\mu_s'$. The term $q_0(\mathbf{r}-\mathbf{r}_0)$ is the isotropic source located at $\mathbf{r}=\mathbf{r}_0$. If we assume that the medium is purely viscous, then the scattering particles are pictured to diffuse through the medium. For a viscous medium, the mean-square displacement suffered by the particle at $\mathbf{r}$, denoted $\langle \Delta r^2(\mathbf{r},\tau)\rangle$, has a linear time evolution given by $\langle \Delta r^2(\mathbf{r},\tau)\rangle = 6D_B(\mathbf{r})\tau$ [3,12], where $D_B(\mathbf{r})$ is the time-independent particle diffusion coefficient related to the viscosity η of the medium. We use the mixed boundary condition to solve the propagation equation (2.1) for $G(\mathbf{r},\tau)$:

$$D(\mathbf{r})\frac{\partial G(\mathbf{r},\tau)}{\partial \mathbf{n}} = -G(\mathbf{r},\tau), \tag{2.2}$$

on the boundary, $\partial\Omega$. This implies that the light input is only from the source at $\mathbf{r}_0$. Note that when $\tau=0$, Eqs. (2.1) and (2.2) reduce to the propagation equation of photon flux of DOT.

We denote $A=2\mu_s' k_0^2$ and $f=D_B$. In a practical experiment, the measurement on the boundary is not the field $G(\mathbf{r},\tau)$, but a quantity related to $|g_1(\mathbf{r},\tau)| = |G(\mathbf{r},\tau)/G(\mathbf{r},0)|$, namely, the intensity autocorrelation given by [4,13]

$$\langle I(\mathbf{r},\tau) I(\mathbf{r},t+\tau)\rangle \equiv g_2(\mathbf{r},\tau) = 1 + \gamma |g_1(\mathbf{r},\tau)|^2. \tag{2.3}$$

Here γ is a constant dependent on the collection optics used in the experiments.

However, the inverse problem presented here attempts to find the particle diffusion coefficient f using the boundary measurement of $G(\mathbf{r},\tau)$ and the forward model by posing it as a minimization problem. Toward this, we first establish the existence of solution of the forward operator and its Fréchet derivative. Thereafter the conditions for the objective functional containing the mean-square error between the computed and the experimental measurements and a regularization term to have a local minimum are established. The Newton algorithm to reach this minimum and its convergence are also established.

A. Solution of Forward Equation for Gaussian Source: Notation

Let Ω be an open subset of $\mathbb{R}^n$, $n \geqslant 2$, and f be the function to be reconstructed with a known background value f'. Let Ω' be the region fully contained in Ω such that f equals the background value f' outside Ω'. That is $f=f'+\rho$ with supp $\rho \subset \Omega'$, where $\Omega' \subset\subset \Omega$. Thus Ω' is the region of interest for the reconstruction of f. The notation $\Omega' \subset\subset \Omega$ means that Ω' is open and $\overline{\Omega'} \subset \Omega$ and supp f is the support of f.

B. Existence of Forward Solution

We assume the source q_0 to be an isotropic Gaussian source [i.e., $q_0 \in L^2(\Omega)$] located at a distance of one transport mean free path (typically 1 mm) inside the tissue. Let V be the space of $H^1(\Omega)$ functions, but with the inner product defined as

$$\langle G, \psi\rangle = \langle \nabla G, \nabla \psi\rangle_{L^2(\Omega)} + \langle G|_{\partial\Omega}, \psi|_{\partial\Omega}\rangle_{L^2(\partial\Omega)} \tag{2.4}$$

with the induced norm

$$\|G\|_V = [\|\nabla G\|^2_{L^2(\Omega)} + \|G|_{\partial\Omega}\|^2_{L^2(\partial\Omega)}]^{1/2}.$$

Consider the weak formulation of Eqs. (2.1) and (2.2) given by

$$\int_\Omega D\nabla G\cdot\nabla\psi+\int_{\partial\Omega} G\psi+\int_\Omega(\mu_a+Af\tau)G\psi=\int_\Omega q_0\psi, \tag{2.5}$$

where $G,\psi\in V$. Define the bilinear and linear forms in $V\times V$ and V, respectively, by

$$B(G,\psi)=\int_\Omega D\nabla G\cdot\nabla\psi+\int_{\partial\Omega} G\psi+\int_\Omega(\mu_a+Af\tau)G\psi,$$

$$L(\psi)=\int_\Omega q_0\psi.$$

We remark that $\|.\|_V$ is equivalent to $\|.\|_{H^1(\Omega)}$. Using Holders inequality, one can show that the bilinear form $B(G,\psi)$ is bounded and satisfies the coercivity condition. Also, L is a bounded linear operator defined on V for $q_0\in L^2(\Omega)$ and hence by the Lax–Milgram lemma [14], there is a unique G, which satisfies the weak formulation (2.5). Further, we have

$$\|G\|_V\leq C\|q_0\|_{L^2(\Omega)}$$

for an appropriate finite constant C. Because of the interior regularity [15] of G in $\Omega'\subset\subset\Omega$, we get $G|_{\Omega'}\in H^2(\Omega')$ and, further, there is a constant C such that

$$\|G\|_{H^2(\Omega')}\leq C\|q_0\|_{L^2(\Omega)}.$$

3. FRÉCHET DERIVATIVE

In the forward propagation equation (2.1) for the basic quantity $G(\mathbf{r},\tau)$, we perturb $f(\mathbf{r})$ to $f(\mathbf{r})+f^\delta(\mathbf{r})$ and obtain a perturbation in $G(\mathbf{r},\tau)$ by $G^\delta(\mathbf{r},\tau)$. Substituting these into Eq. (2.1), after simplification, we get the equation connecting $G^\delta(\mathbf{r},\tau)$ to $f^\delta(\mathbf{r})$, which we call the Fréchet derivative of the forward propagation equation:

$$\nabla\cdot D\nabla G^\delta(\mathbf{r},\tau)-(\mu_a+Af\tau)G^\delta(\mathbf{r},\tau)=Af^\delta\tau G \tag{3.1}$$

with the boundary condition

$$G^\delta(\mathbf{r},\tau)+D\frac{\partial G^\delta(\mathbf{r},\tau)}{\partial\mathbf{n}}=0. \tag{3.2}$$

The existence and uniqueness of solution of the above equation can also be proved by using the standard weak formulation and subsequent application of the Lax–Milgram lemma. For Gaussian source excitation, the right-hand side of Eq. (3.1) has to be in $L^2(\Omega)$ which is true if we assume that $f^\delta\in L^2(\Omega)$ and the supp$f^\delta\subset\Omega'$. As remarked above, we have the interior regularity that $G|_{\Omega'}\in H^2(\Omega')$, and for $n=2,3$, we use the imbedding $H^2(\Omega')\hookrightarrow C(\Omega')$ to get $G|_{\Omega'}\in C(\Omega')$. Thus $Af^\delta G\in L^2(\Omega)$, and via the standard weak formulation we get $G^\delta\in H^1(\Omega)$. Moreover, G^δ also satisfies the interior regularity that $G^\delta|_{\Omega'}\in H^2(\Omega')$ and

$$\|G^\delta\|_{H^2(\Omega')}\leq C\|G\|_{C(\Omega')}\|f^\delta\|_{L^2(\Omega')} \tag{3.3}$$

for a finite constant C.

Adjoint of the Fréchet Derivative. Let $G^*\in H^1(\Omega)$ solve the adjoint of the Fréchet derivative of the forward equation given by

$$\nabla\cdot D\nabla G^*-(\mu_a+Af\tau)G^*=0 \tag{3.4}$$

with the boundary condition

$$G^*+D\frac{\partial G^*}{\partial n}=\phi,$$

where $\phi\in L^2(\partial\Omega)$.

Making use of the weak formulation applied to the adjoint equation, we have

$$\|G^*\|_{H^1(\Omega)}\leq C\|\phi\|_{L^2(\partial\Omega)}.$$

Using the interior regularity of the equation, we have

$$\|G^*\|_{H^2(\Omega')}\leq C\|\phi\|_{L^2(\partial\Omega)}.$$

Now using the imbedding $H^2(\Omega')\hookrightarrow C(\Omega')$, we get

$$\|G^*\|_{L^\infty(\Omega')}\leq K_1\|\phi\|_{L^2(\partial\Omega)}.$$

Here K_1 is a suitable finite constant. Assume a Gaussian source excitation and hence $G^\delta\in H^1(\Omega)$, and thus $G^\delta|_{\partial\Omega}\in H^{1/2}(\partial\Omega)$. With this, define the map $DF(f)$ by

$$DF(f)(f^\delta)=G^\delta(\mathbf{r},\tau)|_{\partial\Omega}.$$

Thus $DF(f)(f^\delta)$ indicates the changes in the boundary values of the field for a change f^δ from the background value f. Using the standard definition of the adjoint, we see that

$$DF^*(f)(\phi)=A\tau GG^*|_{\Omega'}.$$

Note that we treat functions in $L^2(\Omega')$ as functions of $L^2(\Omega)$ by extending them to zero outside Ω'.

4. APPROXIMATE SOLUTION OF INVERSE PROBLEM BY REGULARIZED LEAST SQUARE MINIMIZATION

The field autocorrelation $G(\mathbf{r},\tau)$ depends on the particle diffusion coefficient f, and therefore we write $G(\mathbf{r},\tau)=G(\mathbf{r},\tau,f)$ to show this dependence. The inverse problem can be stated as follows: given the measurements $G(\mathbf{r},\tau,f)$ on the boundary $\partial\Omega$, find f over Ω. Clearly, this problem is nonlinear and ill posed, which is usually resolved by stating it as an optimization problem. We seek a minimizer f^* for an objective functional Θ over an admissible class of f in which $G(\mathbf{r},\tau,f)$ satisfies the forward problem given in Eq. (2.1). Define the forward map $F(f)$ over $\mathrm{Dom}(F)\subset L^\infty(\Omega)$ as

$$F(f)=G(\mathbf{r},\tau)|_{\partial\Omega}.$$

With $f\in L^\infty(\Omega)$ and $q_0\in L^2(\Omega)$, we have $G\in H^1(\Omega)$, which implies $G|_{\partial\Omega}\in H^{1/2}(\partial\Omega)$. Let m^e be the measurement $G|_{\partial\Omega}$ corresponding to a particular particle diffusion coefficient f to be reconstructed. For an initial guess $f=f'$, we define the objective functional $\Theta(\rho)$ as

$$\Theta(\rho)=\frac{1}{2}\|F(\tilde{\rho}+f')-m^e\|^2_{L^2(\partial\Omega)}+\frac{\beta}{2}\|\rho\|^2_{L^2(\Omega')}. \tag{4.1}$$

We would like to minimize $\Theta(\rho)$ over an admissible class of ρ, i.e., $\min_{\rho\in L^2(\Omega')}\Theta(\rho)$. Here β is the Tikhonov regularization parameter and $\tilde{\rho}=\rho$ in Ω', $\tilde{\rho}=0$ in $\Omega\setminus\Omega'$. We expand $\Theta(\rho)$ in terms of a Taylor series about ρ up to the second-order differential:

$$\Theta(\rho+\delta\rho)=\Theta(\rho)+D\Theta(\rho)(\delta\rho)+\frac{1}{2}D^2\Theta(\rho)(\delta\rho,\delta\rho). \tag{4.2}$$

Here $D\Theta(\rho)(\delta\rho)$ is the differential of $\Theta(\rho)$ in the direction $\delta\rho$. As explained above, f can be expressed as $f=\rho+f'$, where f' defined on $\Omega\setminus\Omega'$ is known to us. Perturbation in f, denoted f^δ, is carried out through ρ as $\delta\rho$ in Ω' only. The derivative of $\Theta(\rho)$ in the direction $\delta\rho$, $D\Theta(\rho)(\delta\rho)$, is [16]

$$D\Theta(\rho)(\delta\rho)=\langle\phi,DF(\rho+f')(\delta\rho)\rangle+\beta\langle\rho,\delta\rho\rangle, \tag{4.3}$$

where $\phi=F(\tilde{\rho}+f')-m^e$. We also have

$$\langle\phi,DF(\rho+f')(\delta\rho)\rangle=A\tau\langle\delta\rho,DF^*(\rho+f')(\phi)\rangle.$$

Substituting the above expression into Eq. (4.3), we have the first-order derivative of $\Theta(\rho)$ in the direction $\delta\rho$:

$$D\Theta(\rho)(\delta\rho)=A\tau\langle DF^*(\rho+f')(\phi)+\beta\rho,\delta\rho\rangle.$$

Define the gradient Gr of the objective functional as

$$Gr(\rho)=DF^*(\rho+f')[F(\rho+f')-m^e]+\beta\rho. \tag{4.4}$$

In a similar manner, we can derive the second-order differential of $\Theta(\rho)$. Neglecting the second-order differential term of the adjoint map, $D^2F^*(f)(\phi)$, we have

$$D^2\Theta(\rho)(\delta\rho,\delta\rho)=\langle DF^*(\rho+f')DF(\rho+f')(\delta\rho)+\beta\delta\rho,\delta\rho\rangle.$$

Define the Hessian as

$$H(\rho)(\delta\rho)=DF^*(\rho+f')DF(\rho+f')(\delta\rho)+\beta\delta\rho. \tag{4.5}$$

The gradient $Gr(\rho)$ and the Hessian $H(\rho)(\delta\rho)$ are connected through the linear system of equations

$$H(\rho)(\delta\rho)=-Gr(\rho). \tag{4.6}$$

This can be solved iteratively for ρ by using the Gauss–Newton method given by

$$\rho_{i+1}=\rho_i-H(\rho_i)^{-1}Gr(\rho_i). \tag{4.7}$$

The objective functional $\Theta(\rho)$ defined on $\mathrm{Dom}(\Theta)\subset L^2(\Omega')$ has a minimizer if certain conditions are imposed on Θ and $\mathrm{Dom}(\Theta)$. Specifically, we look for a weakly closed domain over which Θ is defined, thus ensuring the weak limits to be in $\mathrm{Dom}(\Theta)$. We assume that the objective functional Θ is weakly lower semicontinuous, which is required in order to prove the existence of its minimizer.

Theorem 4.1. *Let* $A=\{\rho\in L^2(\Omega'):\rho+f'\geq a>0\}$ *and assume that the functional* Θ *is weakly lower semicontinuous. Then* Θ *has a minimizer* ρ_β *in* A.

Proof. Let $\{\rho_i\}\subset A$ with $\Theta(\rho_i)\to M_\beta=\inf\{\Theta(\rho):\rho\in A\}$. Then, by definition of M_β, for any $n\in\mathbb{N}$, there is an index i_n such that

$$\Theta(\rho_{i_n})\leq M_\beta+\frac{1}{n}\leq M_\beta+1. \tag{4.8}$$

Thus we have

$$\frac{\beta}{2}\|\rho_{i_n}\|_{L^2(\Omega')}\leq\Theta(\rho_{i_n})\leq M_\beta+1.$$

Consider the set $A\cap\{\|\rho\|_{L^2(\Omega')}\leq(2/\beta)(M_\beta+1)\}$, which is closed and bounded and hence weakly compact in $L^2(\Omega)$. So the sequence ρ_{i_n} has a convergent subsequence, again denoted ρ_{i_n}, which converges weakly to some ρ_β, such that $\|\rho_\beta\|_{L^2(\Omega')}\leq(2/\beta)(M_\beta+1)$ and $\rho_\beta\in A$. The last inequality is derived by using the fact that the norm is weakly lower semicontinuous.

If the function Θ is weakly lower semicontinuous, then

$$\Theta(\rho_\beta)\leq\liminf\Theta(\rho_{i_n})\leq M_\beta+\frac{1}{n}.$$

Now, as $n\to\infty$, we see that $\Theta(\rho_\beta)\leq M_\beta$. Since $\rho_\beta\in A$, we get $\Theta(\rho_\beta)=M_\beta$, which proves the theorem. □

The weak lower semicontinuity assumption needed for the existence of the minimizer is valid if the Hessian of the functional Θ is positive semidefinite as stated in the following theorem.

Theorem 4.2. *Let the functional* $\Theta:A\subset L^2(\Omega')\to\mathbb{R}$ *be twice Gateaux differentiable at every point and in all directions in* A. *Let the gradient* $Gr(\rho)$ *of the objective functional* Θ *be defined for all* $\rho\in A$. *If the second Gateaux derivative* $D^2\Theta(\rho)(\delta\rho,\delta\rho)$ *is positive semi-definite, i.e*,

$$D^2\Theta(\rho)(\delta\rho,\delta\rho)\geq 0\qquad\forall\,\rho,\delta\rho\in A,\quad\delta\rho\neq 0, \tag{4.9}$$

then the functional Θ *is weakly lower semicontiuous in* A.

For the standard proof of the above theorem one can refer to [17]. The above condition on the second Gateaux derivative is equivalent to saying that the Hessian should be positive semidefinite on A, i.e.,

$$D^2\Theta(\rho)(\delta\rho,\delta\rho)=\langle H(\rho)(\delta\rho),\delta\rho\rangle\geq 0\qquad\forall\,\rho,\delta\rho\in V,\quad\delta\rho\neq 0. \tag{4.10}$$

A. Discretized Gauss–Newton Scheme for Inversion

Discretization of the forward problem gives us a system of equation $\mathbf{m}^e=\mathcal{F}(\boldsymbol{\rho})$, where $\mathbf{m}^e$ is a partial set of noisy measurements on the boundary assumed to be available on boundary nodes, $\boldsymbol{\rho}$ is the discretized parameter vector to be reconstructed, which in our case is $\mathbf{D_B}$, and $\mathcal{F}$ is a bounded operator obtained from Eq. (2.1). The Gauss-Newton algorithm (4.7) is

$$\mathbf{D}_\mathbf{B}^{i+1}=\mathbf{D}_\mathbf{B}^i-(J^TJ(\mathbf{D}_\mathbf{B}^i)+\lambda I)^{-1}J^T(\mathbf{D}_\mathbf{B}^i)\Delta\mathbf{m}_i. \tag{4.11}$$

Here $J^TJ(\mathbf{D}_\mathbf{B}^i)$ is the approximation to the Hessian evaluated at the current estimate of the property $\mathbf{D}_\mathbf{B}^i$, $J^T(\mathbf{D}_\mathbf{B}^i)\Delta m_i$ is a gradient of $\mathcal{F}(\mathbf{D}_\mathbf{B}^i)$, and $\Delta\mathbf{m}_i=\mathbf{m}^e-\mathbf{m}^i$ with $\mathbf{m}^i$ being the computed measurement through $\mathbf{D}_\mathbf{B}^i$ and $J(\mathbf{D}_\mathbf{B}^i)$ the Jacobian evaluated at $\mathbf{D}_\mathbf{B}^i$. The term λI is added for regularization, where λ is the regularization parameter. To continue the algorithm of Eq. (4.11) the Hessian and gradient are recomputed. The stopping criterion for the iteration is that $\|\Delta\mathbf{m}_i\|<\epsilon$, where ϵ is a preset small bound for the error.

The Jacobian should be evaluated for the particular measurement made at the boundary, which is $\mathbf{m}\equiv g_2(\tau)$. Since $G(\mathbf{r},0)$, the intensity, can also be measured, we define a measurement operator $\mathcal{M}$ acting on $G(\mathbf{r},\tau)$ as [see Eq. (2.3)]

$$\mathcal{M}\{G(\mathbf{r},\tau)\}\equiv G^2(\mathbf{r},0)\left(\frac{\mathbf{m}-1}{\gamma}\right)\equiv\Gamma(\mathbf{r},\tau) \tag{4.12}$$

with $\mathbf{r}\in\partial\Omega$. The Jacobian for this measurement, $\Gamma(\mathbf{r},\tau)$, can be computed by using Eqs. (3.1) and (3.4) [4]:

$$\left\{\frac{\partial\Gamma(r_i,\tau)}{\partial D_B^{\delta}(r_j)}\right\} = \mathrm{Re}\{2\mu_s' k_0^2 \tau \bar{G}(r_i,\tau) G_R^{\phi}(r_j,r_i,\tau) G(r_j,\tau)\}. \tag{4.13}$$

Here $G_R^{\phi}(\mathbf{r},\tau)$ solves the adjoint equation (3.4).

5. PSEUDODYNAMICAL APPROACH TO RECONSTRUCTION

The Gauss–Newton algorithm of Eq. (4.11) requires the modification introduced by the regularization term because the system matrix $J^T J$ usually has a large null space and cannot be inverted as it is. An alternative to the Gauss–Newton algorithm is provided by quasi-Newton method wherein the inverse of the Hessian is approximated from knowledge of the gradient of the objective functional. However, for the quasi-Newton method the rate of convergence is smaller. The addition of the regularization term (or the regularization operator) also alters the minimization problem we originally intended solving. We note that while an optimal choice of the regularization parameter leads to meaningful solutions, even small variations in the parameter can result in unacceptably large errors.

An alternative route to the above iterative solution is through introducing an artificial dynamics into the system and treating the steady-state response of the artificially evolving dynamical system as a solution. This alternative also avoids an explicit inversion of the linearized operator in the Gauss–Newton update equation. Thus, we introduce an artificial dynamics to the Gauss–Newton update equation (4.11). We remark that the "time" used here is a pseudo-variable, and the numerical integration of the resulting ODE will lead us to the solution ρ^* that minimizes the functional Θ in Eq. (4.1).

To show this, we rewrite Eq. (4.11), keeping $\lambda = 0$ (the regularization parameter) as a linearized ODE in continuous time [18,19]. Thus, we have

$$\dot{\mathbf{D}}_\mathbf{B} + M(\mathbf{D}_\mathbf{B}^0)(\mathbf{D}_\mathbf{B}(t) - \mathbf{D}_\mathbf{B}^0) + V(\mathbf{D}_\mathbf{B}^0) = 0, \tag{5.1}$$

where $M(\mathbf{D}_\mathbf{B}) = [J^T(\mathbf{D}_\mathbf{B}) J(\mathbf{D}_\mathbf{B})]$, $V(\mathbf{D}_\mathbf{B}) = J^T(\mathbf{D}_\mathbf{B})(\mathbf{m}^e - \mathbf{m}(\mathbf{D}_\mathbf{B}^0))$ and $\dot{\mathbf{D}}_\mathbf{B}$ represents time derivative of $\mathbf{D}_\mathbf{B}$. Further, $\mathbf{D}_\mathbf{B}^0$ is the linearization point that at the start of the algorithm may be taken as the background value, which is assumed to be known.

Indeed, Eq. (5.1) is an approximation, as it is the linearized version of the nonlinear problem. See the remarks below. First we show that $\mathbf{D}_\mathbf{B}(t)$ converges to $\mathbf{D}_\mathbf{B}^* = \rho^*$, the minimal solution, as $t \to \infty$, assuming the model is exact. Remark 3 below gives a suggestion as to the actual implementation.

Equation (5.1) on integration over $(0,t]$ becomes

$$\mathbf{D}_\mathbf{B}(t) = \exp([-M(\mathbf{D}_\mathbf{B}^0)](t))(\mathbf{D}_\mathbf{B}^0(t)) + \int_0^t \exp(-M(\mathbf{D}_\mathbf{B}^0)(t-s)) f(s) ds, \tag{5.2}$$

where $f(t) = M(\mathbf{D}_\mathbf{B}^0)\mathbf{D}_\mathbf{B}^0 - V(\mathbf{D}_\mathbf{B}^0)$.

That is, we get

$$\mathbf{D}_\mathbf{B}(t) = \exp([-M(\mathbf{D}_\mathbf{B}^0)](t))(\mathbf{D}_\mathbf{B}^0(t)) + M(\mathbf{D}_\mathbf{B}^0)^{-1}(M(\mathbf{D}_\mathbf{B}^0)\mathbf{D}_\mathbf{B}^0 - V(\mathbf{D}_\mathbf{B}^0)). \tag{5.3}$$

But $\mathbf{D}_\mathbf{B}^*$ satisfies $M(\mathbf{D}_\mathbf{B}^0)\mathbf{D}_\mathbf{B}^0 - V(\mathbf{D}_\mathbf{B}^0) = M(\mathbf{D}_\mathbf{B}^0)\mathbf{D}_\mathbf{B}^*$.

Thus Eq. (5.3) becomes

$$\mathbf{D}_\mathbf{B}(t) = \exp([-M(\mathbf{D}_\mathbf{B}^0)](t))(\mathbf{D}_\mathbf{B}^0(t)) + \mathbf{D}_\mathbf{B}^*, \tag{5.4}$$

which converges to $\mathbf{D}_\mathbf{B}^*$ as $t \to \infty$. Note that we have assumed that $M(\mathbf{D}_\mathbf{B}^0)$ is positive definite. Therefore, we have the following theorem.

Theorem 5.1. *If $M(\mathbf{D}_\mathbf{B}^0) = J^T J(\mathbf{D}_\mathbf{B}^0)$ is positive definite, the pseudo-time marching scheme leads to a solution $\mathbf{D}_\mathbf{B}(t)$ that tends to $\mathbf{D}_\mathbf{B}^*$.*

Remark 1. It is also observed that the step size in the pseudo-time recursion regularizes the updates so that spurious oscillations in them due to the near-zero singular values of the associated coefficient matrix are largely removed. This assumes great significance when dealing with insufficient data generated from a practical setup using reflection geometry, leading to severely ill-conditioned matrices in the reconstruction step. Moreover, the exponential form of the updates admits exploitation of powerful concepts in Lie group theory, such as Trotter's formula [20] or Magnus expansion, so that an additional level of numerical stabilization is possible through the preservation of certain invariants. The last aspect has, however, been kept outside the scope of the present work.

Remark 2. As mentioned above, Eq. (5.1) is a linearized approximation of a nonlinear system, and hence Eq. (5.1) may be valid only for a small time. Thus a large-time integration may not represent the actual solution. In other words, the approximation is valid only locally around the linearization point. Therefore, to get a more accurate solution in an application, one needs to integrate over small time steps Δt leading to an update of $\mathbf{D}_\mathbf{B}^0$ and a relinearization of the nonlinear equation by estimating J and Δm at the current property distribution at Δt. We note that for the convergence of the recursion, the positive definiteness of $J^T J$ has to be ensured at the end of each time step.

Remark 3. The requirement that $J^T J$ be positive definite at the initial guess of $\mathbf{D}_\mathbf{B}$, namely, at $\mathbf{D}_\mathbf{B}^0$, is not usually met and also cannot be demanded. As is done in the earlier work on an inverse problem using Newton iteration [21], it is, at the most, reasonable to assume positive definiteness of $J^T J$ at the optimal point $\mathbf{D}_\mathbf{B}^*$. Thus, if the initial guess is very close to $\mathbf{D}_\mathbf{B}^*$, then positive definiteness will be available because of the continuity of $J^T J$. As far as numerical implementation is concerned, we start the algorithm with a regularization term λI. More precisely, we consider $J^T J(\mathbf{D}_\mathbf{B}^0) + \lambda I$ instead of $J^T J(\mathbf{D}_\mathbf{B}^0)$. We update $D_\mathbf{B}^0$, successively to $\mathbf{D}_\mathbf{B}^1, \mathbf{D}_\mathbf{B}^2, \ldots$ at small intervals $\Delta t, 2\Delta t \ldots$.

Finally, we have the algorithm derived from Eq. (5.3) as

$$\Delta\mathbf{D}_\mathbf{B}^{i+1} = \exp([-(M(\mathbf{D}_\mathbf{B}^i) + \lambda I)\Delta t])\mathbf{D}_\mathbf{B}^i + \int_{t_i}^{t_i+\Delta t} \exp([-(M(\mathbf{D}_\mathbf{B}^i) + \lambda I)])(t_i + \Delta t - s) f(s) ds,$$

$$\mathbf{D}_\mathbf{B}^{i+1} = \mathbf{D}_\mathbf{B}^{i} + \Delta\mathbf{D}_\mathbf{B}^{i+1} \tag{5.5}$$

Here $f(t)$ is redefined to nullify the effect of regularization by adding an additional term to $V(t)$ as follows: $V(\mathbf{D}_\mathbf{B}^i) = J^T(\mathbf{D}_\mathbf{B}^i)(\mathbf{m}^e - \mathbf{m}(\mathbf{D}_\mathbf{B}^i)) + \lambda(\mathbf{D}_\mathbf{B}^i - \mathbf{D}_\mathbf{B}^0)$, similar in spirit to the Levenberg–Marquardt method [7,8].

As $\mathbf{D_B}$ approaches $\mathbf{D}_\mathbf{B}^*$, J^TJ becomes positive definite and hence the relevance of the regularization parameter is minimal and can be ignored. This phenomenon is amply demonstrated in our numerical simulations. Thus in our computations, we begin with a regularization parameter and with the new update Eqs. (5.5) the contribution of λ decreases to zero as the true solution is approached.

6. NUMERICAL EXPERIMENTS

Before we proceed with proving the efficacy of the algorithm through numerical simulations, a word on limitations brought in by data collection geometry in a practical experimental scenario. In the DCT imager a diffuse reflection geometry is used for data gathering [3], wherein the light source and a set of detectors, with the detector fibres prealigned to receive a single speckle, are fixed at selected distances so that a certain tissue volume at a desired depth is covered by all the source–detector pairs. A smaller data set from the DCT imager leads to a severely underdetermined reconstruction problem, leading to numerical difficulties, particularly for the Newton algorithm requiring an inversion of an ill-conditioned and rank-deficient matrix. It is here that pseudo-time recursion, which avoids matrix inversion, provides an alternative acceptable route for reconstruction.

The object used in our numerical simulations is circular, taken as the cross section of a cylinder of diameter 8 cm. The background optical and mechanical properties are kept as $\mu_a^b = 0.001\ \text{cm}^{-1}$, $\mu_s'^b = 8\ \text{cm}^{-1}$ and $D_B^b = 1 \times 10^{-8}\ \text{cm}^2/\text{s}$. There are two circular inhomogeneous inclusions, which are D_B inhomogeneities, with diameter 1.4 cm each, one with a value of $D_B = 0.25 \times 10^{-8}\ \text{cm}^2/\text{s}$ at $(-2.5\ \text{cm}, 0\ \text{cm})$, and the other with a value of $D_B = 0.75 \times 10^{-8}\ \text{cm}^2/\text{s}$ at $(2.5\ \text{cm}, 0\ \text{cm})$ (The object is assumed to be centered at the origin of the coordinate axes). Therefore the inclusion in the background is

$$D_B(x,y) = \begin{cases} 0.25 \times 10^{-8}\ \text{cm}^2/\text{s} & \text{if } \sqrt{(x+2.5)^2 + (y)^2} \leqslant 0.7 \\ 0.75 \times 10^{-8}\ \text{cm}^2/\text{s} & \text{if } \sqrt{(x-2.5)^2 + (y)^2} \leqslant 0.7 \end{cases}.$$

To generate the experimental data numerically, Eqs. (2.1) and (2.2) are discretized by using the finite element method with 1933 nodes and 3723 triangular linear elements. For a collimated source on the boundary, 40 detectors are placed equiangularly on either side of the diametrically opposite point to the source location, to cover an overall angle of 320°. The discretized forward equation is solved for $G(\mathbf{r}, \tau)$ for $\tau = 10^{-4}$ s. While the experimental data sets are generated, Gaussian noise of varying intensities is added (1%–5%) to $G(\mathbf{r}, \tau)$. Using the noisy $G(\mathbf{r}, \tau)$ and Eq. (4.12), experimentally tenable measurements $\{\Gamma(\mathbf{r}, \tau)\}$ are generated. The above procedure is repeated by rotating the source–detector combination by steps of 10° to gather 36 sets of 40 readings each.

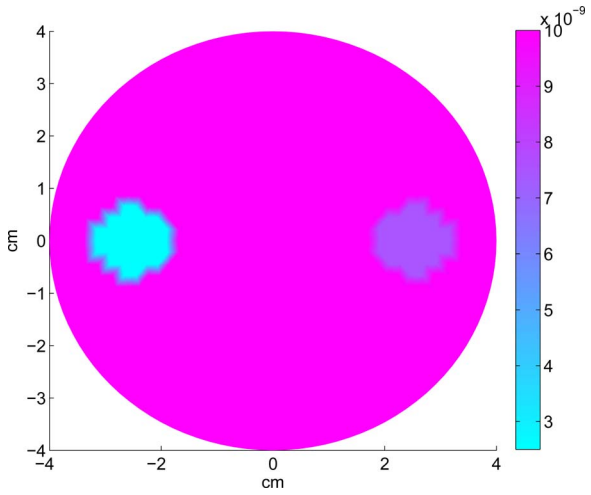

Fig. 1. (Color online) Original particle diffusion coefficient distribution (cm^2/s) used in the simulations

For inversion of data we use a coarser mesh, discretizing the domain with 1243 nodal points and 2376 triangular elements. First we perform reconstruction using the Gauss–Newton algorithm of Eq. (4.7) [Eq. (4.11) in discrete form] starting the reconstruction algorithm with an initial guess of the property D_B^b, which is the background value. The Jacobian for the measurement $\Gamma(\mathbf{r}, \tau)$ is computed by using Eq. (4.13). The new update is obtained by using Eq. (4.11), where we use an appropriate regularization parameter λ set through trial and error. Once the updated D_B is obtained, $J(\mathbf{D}_\mathbf{B}^i)$ and $\Delta\mathbf{m}_i$ terms are recomputed at the new parameter distribution, and Eq. (4.11) is itself updated. Inversion of the updated Eq. (4.11) gives us the current update for D_B to continue the iteration. The algorithm gave stabilized reconstruction of $D_B(\mathbf{r})$ in about 30 iterations. The gray-level plot of the original $\mathbf{D_B}$ distribution is shown in Fig. 1. The recovered $\mathbf{D_B}$ from the measurements with 1% Gaussian noise is shown in Fig. 2 [the gray-level plot in Fig. 2(a) and the cross sections through the centers of the inhomogeneities of the original and the recovered distributions in Fig. 2(b)]. When the percentage of the noise is increased to 2, the algorithm did not converge (even after regularization), and the reconstruction was not able to reveal the location of the inhomogeneities [see Figs. 3(a) and 3(b)].

In the next step we employ the PD approach to recover the particle diffusion coefficient distribution. As mentioned above, we have used the explicit time integration step and used the recursion of Eqs. (5.5) to recover $\mathbf{D_B}$. The algorithm took 15 recursions to give an accurate $\mathbf{D_B}$ recovery for which the mean-square error in the measurement domain reached a minimum. The recovered $\mathbf{D_B}$ distribution for measurement corrupted with 2% noise is shown in Fig. 4 [the gray-level plot in Fig. 4(a) and the cross sections through the centers of the inhomogeneities of the original and the recovered distributions in Fig. 4(b)]. Figures 5(a) and 5(b) are the gray-level plot and the cross-sectional plots of the reconstructed $\mathbf{D_B}$ distributions, respectively, when 5% noise is present in the data.

We also present the reconstruction of absorption coefficient from the boundary measurement of transmitted light, as was done in DOT. This problem can be viewed as

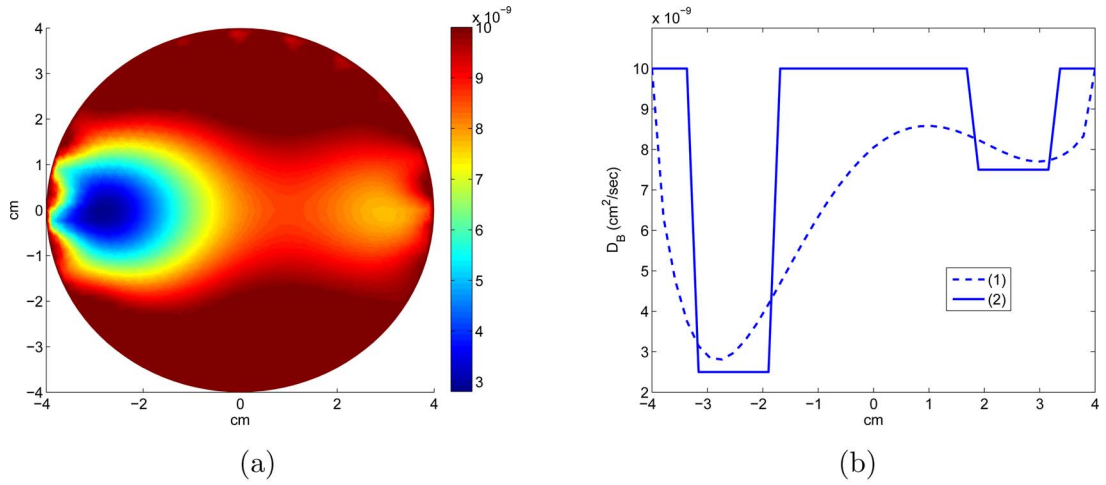

Fig. 2. (Color online) Reconstructed particle diffusion coefficient distribution (cm^2/s) from data with 1% Gaussian noise for the Gauss–Newton method: (a) gray-level-plot and (b) cross-sectional plots through the centers of the inhomogeneities in (a) (dashed curve) as well as the original inhomogeneous object.

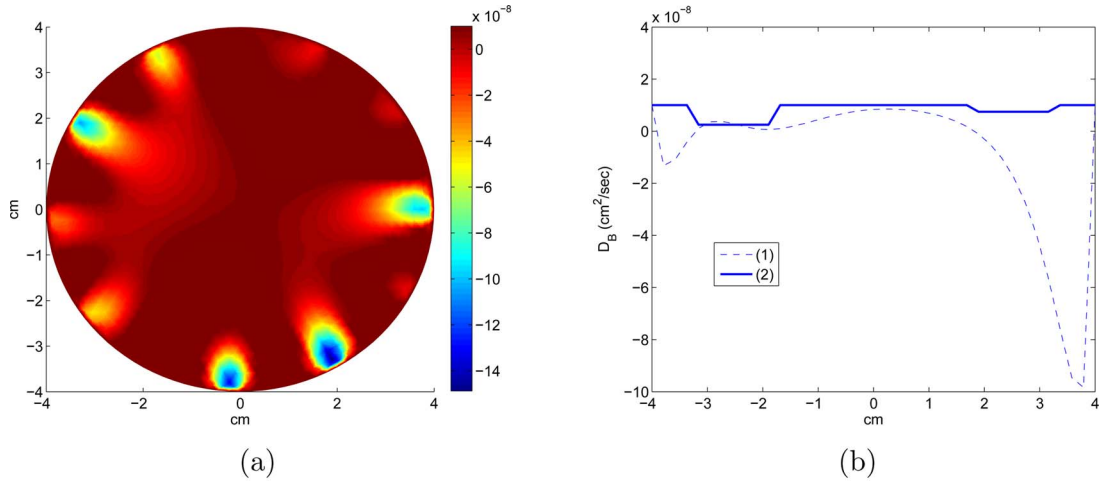

Fig. 3. (Color online) Reconstructed particle diffusion coefficient distribution (cm^2/s) from data with 2% Gaussian noise for the Gauss–Newton method: (a) gray-level plot and (b) cross-sectional plots through the centers of the inhomogeneities in (a) (dashed curve) as well as the original inhomogeneous object.

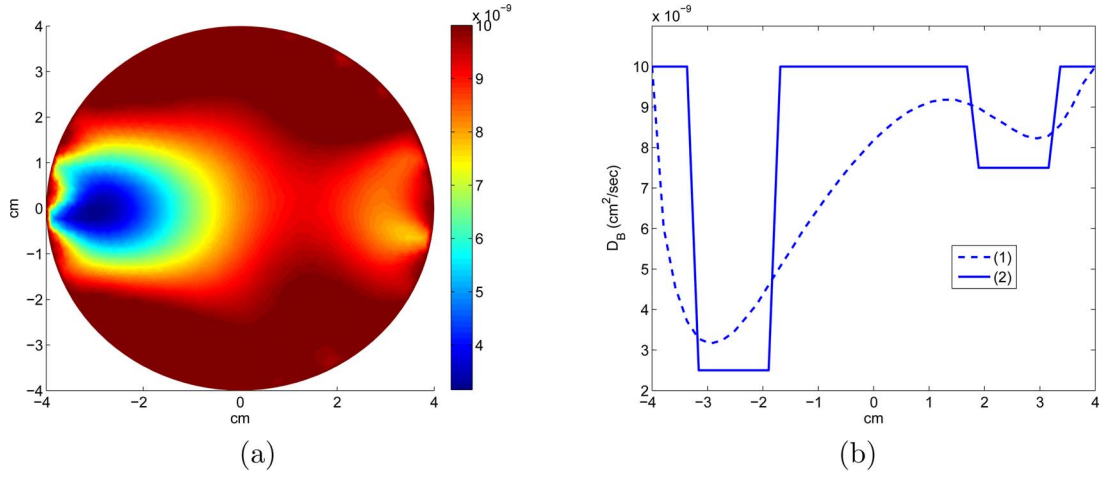

Fig. 4. (Color online) Reconstructed particle diffusion coefficient distribution (cm^2/s) from data with 2% Gaussian noise for the pseudo-time marching scheme: (a) gray-level plot and (b) cross-sectional plots through the centers of the inhomogeneities in (a) (dashed curve) as well as the original inhomogeneous object.

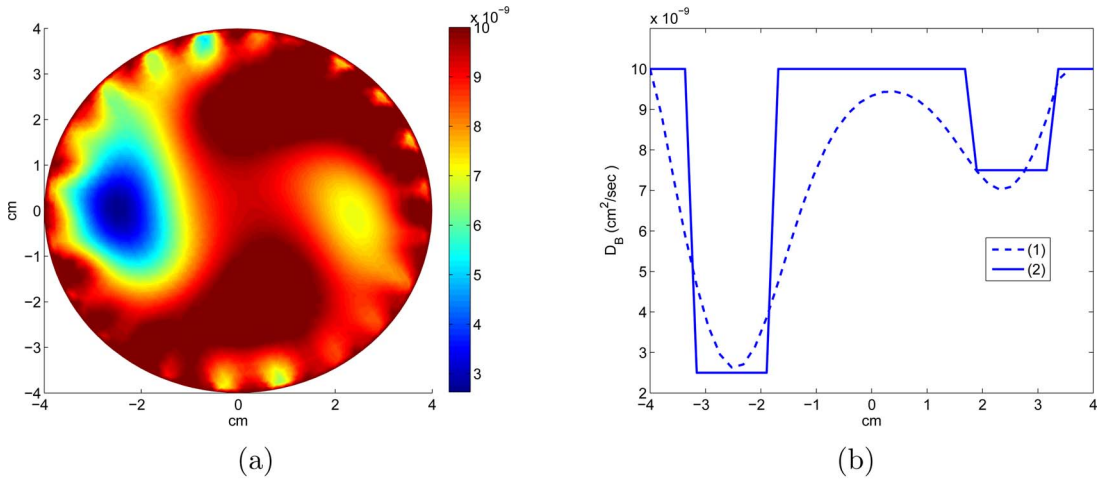

Fig. 5. (Color online) Reconstructed particle diffusion coefficient distribution (cm^2/s) from data with 5% Gaussian noise for the pseudo-time marching scheme: (a) gray-level plot and (b) cross-sectional plots through the centers of the inhomogeneities in (a) (dashed curve) as well as the original inhomogeneous object.

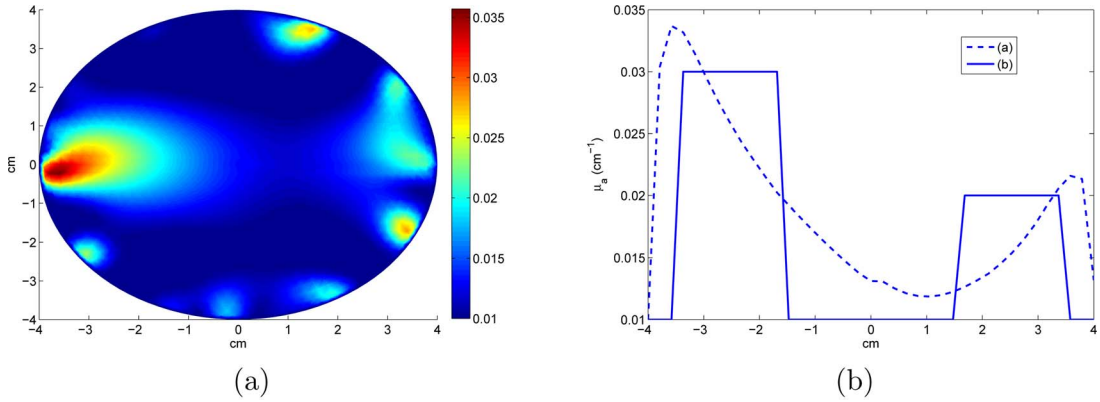

Fig. 6. (Color online) Reconstructed absorption coefficient distribution (cm^{-1}) from data with 5% Gaussian noise for the ordinary Gauss–Newton method: (a) gray-level plot and (b) cross-sectional plots through the centers of the inhomogeneities in (a) (dashed curve) as well as the original inhomogeneous object.

a special case of DWS with $\tau=0$. The object used here is also circular, taken as a cross section of a diffusively scattering cylinder of the same dimensions as earlier. The background optical properties are kept as $\mu_a^b=0.01\ \mathrm{cm}^{-1}$ and $\mu_s'^b=8\ \mathrm{cm}^{-1}$. The inhomogeneous inclusions are also circular, given by,

$$\mu_a(x,y)=\begin{cases}3\times10^{-2}\ \mathrm{cm}^{-1} & \text{if } \sqrt{(x+2.5)^2+(y)^2}\leqslant 0.9\\ 2\times10^{-2}\ \mathrm{cm}^{-1} & \text{if } \sqrt{(x-2.5)^2+(y)^2}\leqslant 0.9\end{cases}.$$

The experimental data used here are $G(\mathbf{r},0)\equiv I(\mathbf{r})$, $\mathbf{r}\in\partial\Omega$ [obtained by solving the forward equation for $G(\mathbf{r},\tau)$ as before] after adding 5% Gaussian noise. The reconstructed μ_a distribution (gray level plot) and a cross section through the centers of the inhomogeneties are shown in Figs. 6(a) and 6(b), respectively, for which Gauss–Newton method has been employed. Reconstruction by using the same data, employing the PD strategy, is shown in Fig. 7 [as before, with the gray-level plot in Fig. 7(a) and the cross sections through the centers of the inhomogeneities of the original and the recovered distributions in Fig. 7(b)].

The results clearly show that the approach using the PD time marching gives reasonably good reconstructions even when the noise is as high as 5%. Moreover, by introducing a matching term to modify the force vector over every recursion step [Eq. (4.11)], we have, for all practical purposes, removed the effect of regularization on the reconstruction at convergence. If we started by setting $\lambda=0$ in Eq. (4.11), the recursion of the PD system generated from it did not give meaningful reconstructions. Instead we used the modification given by Eqs. (5.5). The modified recursion gave good reconstructions, which also effectively nullifies the contribution of the regularization term on convergence. The λ we chose to begin the algorithm is 0.1, and this value is fixed by observing how the data residual error behaves.

7. CONCLUSIONS

We have shown that a pseudo-time marching scheme provides a regularization-insensitive and robust (in the sense of handling noise in data) method to solve the inverse problem of diffuse correlation tomography (DCT) to recover the particle diffusion coefficient from boundary intensity autocorrelation measurement. First a Newton method is set up to solve the mean-square error minimi-

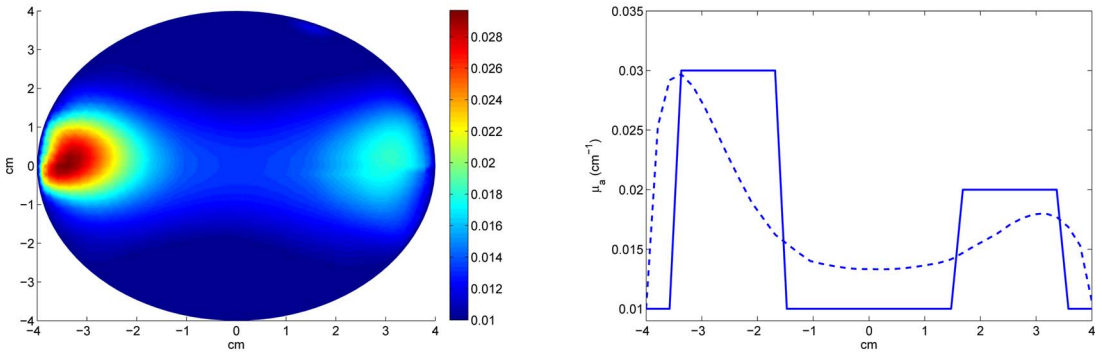

Fig. 7. (Color online) Reconstructed absorption coefficient distribution (cm^{-1}) from data with 5% Gaussian noise for the pseudo-time marching scheme (a) gray-level plot and (b) cross-sectional plots through the centers of the inhomogeneities in (a) (dashed curve) as well as the original inhomogeneous object.

zation problem into which the DCT reconstruction is recast. We prove the existence of the minimizer for the above and establish the convergence of the Gauss–Newton algorithm to this minimum. In doing this we also show the existence and behavior of the solutions of the forward propagation equation for the light autocorrelation and its Fréchet derivative and adjoint. The Gauss–Newton update equation, written as an ODE evolving over pseudo-time, is integrated to arrive at the update vector as its steady-state response. We have proved that the integration of the PD system provides asymptotically stable solutions. Through numerical simulations we establish that the PD method is a regularization-insensitive alternative to the Newton iteration, giving robust reconstructions even when the data noise is up to 5%, which was not possible by using the usual Gauss–Newton iteration.

REFERENCES

1. A. P. Gibson, J. C. Hebden, and S. R. Arridge, "Recent advances in diffuse optical imaging," Phys. Med. Biol. **50**, R1–R43 (2005).
2. D. A. Boas, D. H. Brooks, C. A. Dimarzio, M. Kilmer, R. J. Gaudette, and Q. Zhang,"Imaging the body with diffuse optical tomography," IEEE Signal Process. Mag. **18**, 57–75 (2001).
3. C. Zhou, G. Yu, D. Furuya, J. H. Greenberg, A. G. Yodh and T. Durduran, "Diffuse correlation tomography of cerebral blood flow during cortical spreading depression in rat brain," Opt. Express **3**, 1125–1144 (2006).
4. H. M. Varma, A. K. Nandakumaran, and R. M. Vasu, "Study of turbid media with light: recovery of mechanical and optical properties from boundary measurement of intensity autocorrelation of light," J. Opt. Soc. Am. A **26**, 1472–1483 (2009).
5. S. Sakadzic and L. V. Wang, "Correlation transfer and diffusion of ultrasound-modulated multiply scattered light," Phys. Rev. Lett. **96**, 163902 (2006).
6. A. N. Tikhonov and V. Y. Arsenin, *Solution of Illposed Problems* (Winston, 1997).
7. K. Levenberg,"A method for the solution of certain nonlinear problems in least squares," Q. Appl. Math. **2**, 164–168 (1944).
8. D. W. Marquardt,"An algorithm for least squares estimation of nonlinear parameters," J. Soc. Ind. Appl. Math. **11**, 431–441 (1963).
9. B. Banerjee, D. Roy, and R. M. Vasu, "A pseudo-dynamical systems approach to a class of inverse problems in engineering," Proc. R. Soc. London, Ser. A **465**, 1561–1579 (2009).
10. V. Kolehmainen, S. Prince, S. R. Arridge, and J. P. Kaipio, "State-estimation approach to the nonstationary optical tomography problem," J. Opt. Soc. Am. A **20**, 876–889 (2003).
11. B. Banerjee, D. Roy, and R. M. Vasu, "A pseudo-dynamic sub-optimal filter for elastography under static loading and measurements," Phys. Med. Biol. **54**, 285–305 (2009).
12. D. A. Boas, L. E. Campbell, and A. G. Yodh, "Scattering and imaging with diffuse temporal field correlation," Phys. Rev. Lett. **75**, 1855–1858 (1995).
13. C. Usha Devi, R. S. Bharat Chandran, R. M. Vasu and A. K. Sood, "Measurement of visco-elastic properties of breast tissue mimicking materials using diffusing wave spectroscopy," J. Biomed. Opt. **12**, 034035 (2007).
14. S. Kesavan, *Topics in Functional Analysis and Applications* (New Age International, 2008).
15. D. Gilbarg and N. S. Trudinger, *Elliptic Partial Differential Equations of Second Order* (Springer-Verlag, 1983).
16. D. C. Dobson, "Convergence of a reconstruction method for the inverse conductivity problem," SIAM J. Appl. Math. **52**, 442–458 (1992).
17. J. Cea, *Lectures on Optimization–Theory and Algorithms* (Springer Verlag, 1978).
18. D. Roy, "A numeric-analytic technique for non-linear deterministic and stochastic dynamical systems," Proc. R. Soc. London, Ser. A **457**, 539–566 (2001).
19. D. Roy, "Phase space linearization for non-linear oscillators: deterministic and stochastic systems," J. Sound Vib. **231**, 307–341 (2000).
20. M. C. Valsakumar, "Solution of Fokker–Planck equation using Trotter's formula," J. Stat. Phys. **32**, 545–553 (1983).
21. D. C. Dobson, "Phase reconstruction via nonlinear least-squares," Inverse Probl. **8**, 541–558 (1991).